Available online at www.sciencedirect.com
SCIENCE DIRECT®
Applied Surface Science 250 (2005) 124–134
applied surface science
www.elsevier.com/locate/apsusc

Corrosion resistance study of Fe–Mn–Al–C alloys using immersion and potentiostatic tests

Vanessa F.C. Lins[a,*], Marta Afonso Freitas[b], Evando M. Paula e Silva[c]

[a]*Chemical Engineering Department, Engineering School, Federal University of Minas Gerais, 35, 6th floor, Espírito Santo Street, Zip Code 30160-030, Belo Horizonte, Minas Gerais, Brazil*
[b]*Statistical Department, Federal University of Minas Gerais, Antonio Carlos Avenue, 6627, Belo Horizonte, Minas Gerais, Brazil*
[c]*Center for Management and Strategic Studies, Brazilian Government, Setor Comercial Norte Quadra 2, Edifício Corporate Center 1102, Zip Code 70712-900, Brasilia, Federal District, Brazil*

Received 7 September 2004; received in revised form 25 September 2004; accepted 20 December 2004
Available online 19 January 2005

Abstract

The interaction of the Fe–32.7Mn–6.59Al–1.26Si–0.25C (wt.%) and Fe–32.3Mn–8.54Al–1.31Si–0.54C (wt.%) alloys with the environment was evaluated. Potentiostatic and total immersion tests, planned and analyzed by the statistic model of fixed effects were used for the evaluation of corrosion in gasoline, alcohol fuel, lactic acid solution (40 wt.%), sodium chloride solution (3 wt.%), and boiler water. Potentiostatic tests in 1N H_2SO_4 medium presented that the alloys showed a tendency towards passivation. The role that aluminum and silicon play in alloy corrosion mechanism was discussed.

Keywords: Alloy; Potentiostatic; Acid corrosion; Passivity

1. Introduction

Fe–Mn–Al–Si–C (FMA) alloys are an interesting structural material due to its resistance to oxidation [1] and to wear, presenting also a high strain-hardening rate [2]. The initial research was motivated by the desire to improve the ductility and toughness of the ferritic Fe–Al alloys [3]. The manganese addition makes the Fe–Al system austenitic, and its mechanical properties were improved. The effect of manganese on corrosion resistance is detrimental. Manganese with a low passivity coefficient forms an unstable manganese oxides film, decreases the open circuit potential and increases the corrosion current density [4]. Manganese interacts with sulfur in stainless steels to form manganese sulfides. The morphology and composition of these sulfides can have substantial effects on corrosion resistance, especially pitting resistance [5]. Besides β-Mn phase can cause embrittlement [6]. The effects of silicon addition on the mechanical properties, corrosion resistance and high-temperature oxidation resistance of Fe–Mn–Al–C alloys have been presented by many authors [6–15]. They suggest that silicon has a beneficial effect on the strength,

* Corresponding author. Tel.: +55 31 32381773; fax: +55 31 32381789.
E-mail address: vlins@deq.ufmg.br (Vanessa F.C. Lins).

0169-4332/$ – see front matter © 2004 Elsevier B.V. All rights reserved.
doi:10.1016/j.apsusc.2004.12.040

corrosion and oxidation resistance of steel. Silicon in FMA alloys was suggested to possibly act as a solid solution strengthener [14,16]. The solubility of carbon is higher in the Fe–Mn–Al alloys than in stainless steels, and this element can also contribute to the precipitation hardness in the FMA system [15].

The main restriction to the industrial application of the Fe–Mn–Al–Si–C (FMA) alloys is its poor aqueous corrosion resistance in severely corrosive media [6,17–20]. However, Wang and Beck [7] reported that the Fe–30.5Mn–10.4Al–1.3Si–1.01C alloy presented a marine corrosion resistance higher than the observed for the 18.59Cr–0.63Ni–1.07Ti–0.08C (wt.%) steel. The FMA alloys showed lower cost and density than the brass used in marine boat engine. The corrosion rates of the FMA alloys are higher than the corrosion rates of the AISI 304 steel in some specific environments such as boiling HNO_3, 5 wt.% H_2SO_4, 10 and 40 wt.% $FeCl_3$, 3 wt.% NaCl, and in boiling 50 wt.% acetic acid [21]. So in addition to the good mechanical and physical properties of the FMA alloys, the other main requirements for use of the FMA steels is corrosion resistance in working environments. However, very little information concerning the corrosion behavior of this alloy system is available in the literature. The statistical analysis of the corrosion data was important in order to obtain more precise and reliable results.

The aim of this work is to study the corrosion resistance of the Fe–Mn–Al–Si–C alloy, by using total immersion and potentiostatic tests and statistical analysis, applying the Two-Way Analysis of Variance with fixed effect model, in the following environments: lactic acid, 1N H_2SO_4, gasoline, fuel alcohol, 3 wt.% NaCl, and boiler water.

2. Experimental procedures

The Fe–32.7Mn–6.59Al–1.26Si–0.25C (wt.%), alloy 1, and Fe–32.3Mn–8.54Al–1.31Si–0.54C (wt.%), alloy 2, were melted in an atmospheric induction furnace, with tension of 440 V, maximum power of 100 kW and maximum frequency of 100 kHz. The crucible used in the fusion has 100 kg capacity and dimensions of 500 mm × 210 mm (base) × 240 mm (top). The crucible coating, tundish and taphole were made of a refractory (MgO). The ingot mold was big end up, with transversal square section and made of a nodular cast iron. The mass of ingot was 43.6 kg and the density of the alloy was 6.85 g cm^{-3}. The cylindrical-shaped ingots were homogenized at 1000 °C, for 24 h, and water quenched. The steel samples were heated to 1150 °C for 4 h, and forged in the 920–1130 °C temperature ranges. The produced pieces were hot-rolled [2] (81% reduction in thickness), homogenized at 950 °C, for 2 h and water quenched. The final dimensions of the plates were 15 mm × 20 mm. The specimens were polished on 100–600 grades SiC paper to remove any tarnish film and depleted zones, which were produced during annealing. Then, the plates were degreased and dried. All plates were further polished on 600 grade SiC paper and cleaned with acetone prior to the corrosion tests. The samples submitted to metallography were polished on 240–600 grades SiC paper and chromium oxide, and attacked with Nital.

The total immersion tests were planned using the fixed effect model [22], and are according to the ASTM G-31 standard. The tests were carried out at room temperature, without magnetic stirring. The tests were performed in two stages. The corrosive media used in the first stage of corrosion tests are lactic acid, gasoline, fuel alcohol, 3% (w/w) NaCl, and boiler water. The duration of the immersion tests was 20 days. After the corrosion tests, the samples were submitted to a mechanical cleanliness, and a chemical cleanliness with a commercial solution and Na_2CO_3. The mass loss of the samples was determined.

In the second stage of tests, total immersion tests were performed in 1N H_2SO_4. The immersion test time was 120 h.

Electrochemical polarization curves were obtained using a galvanostat/potentiostat, in a series of potential steps of 20 mV. The electrolyte used was 1N H_2SO_4 solution. The time spent at each potential was constant and the current was often allowed to stabilize prior to changing the potential to the next step. The test solution of 1N H_2SO_4 was made from analytical grade reagents and distilled water.

Eq. (1) was used to calculate the sample size n needed to run the experiments and detect a minimum difference D between two treatment means, with a probability value $1 - \beta$:

$$\phi^2 = \frac{nbD^2}{2a\sigma^2} \quad (1)$$

where ϕ^2 is the statistical parameter value given by operating characteristic curves; D the minimum difference between two treatment means; n the sample size; a the number of levels of factor A; b the number of levels of factor B; σ^2 the variance.

In order to estimate the variance in the first stage of tests, the literature data [23] was used ($\sigma^2 = 0.9253$). Considering the literature results [23], D was estimated in 1 mpy. Therefore, the sample size n calculated with the Eq. (1) should be enough to detect a minimum difference of 1 mpy between two treatment means, with a reasonable probability $1 - \beta$ (usually, one tries to get a n value such that $1 - \beta \geq 0.90$). In Eq. (1), $a = 2$ (two different chemical composition of the alloy), and $b = 5$ (five environments).

Eq. (1) then becomes:

$$\phi^2 = 1.35n \quad (2)$$

In order to use the operating characteristic curves, ϕ values had to be calculated for different sample sizes n. Also a probability of type one error of 5% ($\alpha = 5\%$) was chosen. Sample sizes of 1–5 were used in Eq. (2) and the β values were obtained from the operating characteristic curves (Table 1).

The selected sample size was 4, leading to an acceptable β value of 0.11 (or $1 - \beta = 0.99$) (Table 1).

For the variance estimation in the second stage of tests, the corrosion rates obtained in the first stage for the boiler water and sodium chloride solution were used. Then, the calculated standard deviation was:

$$S = (\Sigma \nu_i S_i^2 / \Sigma \nu_i)^{1/2} \quad (3)$$

where $\nu_i = n_i - 1$, S_i^2 = variance of each casela. The values calculated were $S = 0.3874$ and $S^2 = 0.1501$.

In this case, D was also 1 mpy, $a = 2$ (two different alloys), and the $b = 2$ (two different environment). The calculated value of ϕ^2 was 3.33 n. Assuming a α value of 5%, and varying the sample size from 1 to 4, β was obtained (Table 2). The selected sample size was 3, leading to a probability to accept H_0 when H_0 is true (β) of 2.7%. In other words, the probability to reject H_0 when it is false is 1-β = 97.3%.

Table 1
First stage of tests – β values for sample sizes from 1 to 5

Sample size (n)	ϕ^2	ϕ	ν_1	ν_2	β
1	3.35	1.16	1	0	–
2	2.7	1.64	1	10	0.45
3	4.05	2.01	1	20	0.23
4	5.4	2.32	1	30	0.11
5	6.75	2.6	1	40	–

Table 2
Second stage of tests – β values for sample sizes from 1 to 4

Sample size (n)	ϕ^2	ϕ	ν_1	ν_2	β
1	3.33	1.82	1	0	–
2	6.66	2.58	1	4	–
3	9.99	3.16	1	8	0.027
4	13.32	3.65	1	12	–

3. Results and discussion

After hot-rolled, the microstructures of the Fe–32.7Mn–6.59Al–1.26Si–0.25C and Fe–32.3Mn–8.54Al–1.31Si–0.54C (wt.%) alloys were determined. Fig. 1 shows the longitudinal section of the Fe–32.7Mn–6.59Al–1.26Si–0.25C alloy, which presents the phase austenite. The 0.54% C alloy showed a two-phase structure with austenite and ferrite (Fig. 2).

3.1. First stage of the corrosion tests

The alloys immersed in alcohol presented localized corrosion (pits) from the first day of tests (Fig. 3). The contents of Fe, Mn, Cl^- and SiO_2 in the alcohol solution increased after the immersion tests. This result was an evidence of the iron, manganese and silicon corrosion. The concentration of Fe increased

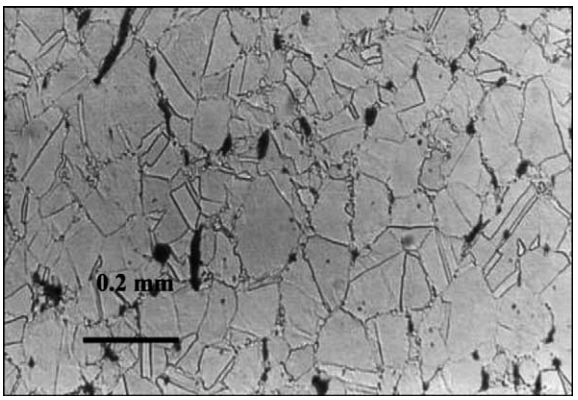

Fig. 1. Longitudinal section of the Fe–32.7Mn–6.59Al–1.26Si–0.25C (wt.%) alloy.

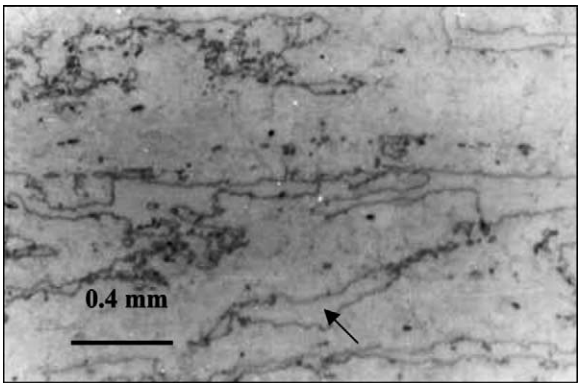

Fig. 2. Longitudinal section of the Fe–32.3Mn–8.54Al–1.31Si–0.54C (wt.%) two-phase alloy. Array indicates the ferrite phase.

from 0.18 to 0.4 mg L^{-1}. The EDS analysis of the pit region showed a sulfur enrichment and the presence of chloride in relation to the composition of alloy (Table 3). The mechanism of pitting corrosion consists of the oxidation of Fe and hydrolysis of $FeCl_2$ in an autocatalytic process.

$$Fe \rightarrow Fe^{2+} + 2e^{-}$$

$$FeCl_2 + 2H_2O \rightarrow Fe(OH)_2 + 2H^{+} + 2Cl^{-}$$

Sulfur enrichment of the pit area can be related with the presence of manganese sulfides that solubilized in the pit area due to the local reduction in pH value.

$$MnS + 2H^{+} \rightarrow Mn^{2+} + H_2S$$

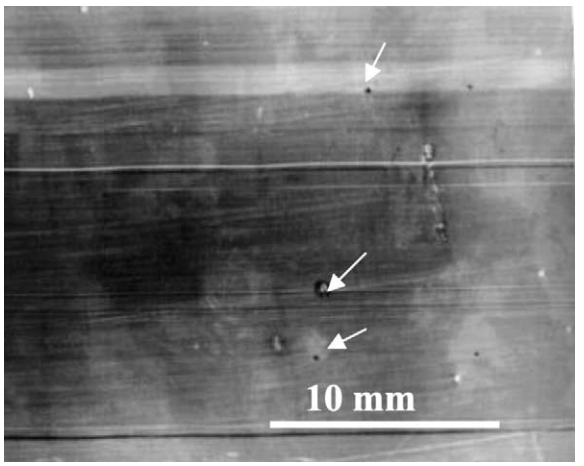

Fig. 3. Surface of Fe–32.3Mn–8.54Al–1.31Si–0.54C alloy after immersion test in alcohol fuel. Arrays indicate corrosion pits.

Table 3
EDS analysis of FMA alloy (alloy 1) after immersion test in alcohol

Element	Inner area of pit (wt.%)	Surface area (wt.%)
Al	9	7
Si	2	1.5
Mn	30	29
Fe	57	61
S	0.8	0.3
Cl	0.3	–

H_2S dissociates in S^{2-} and HS^{-}, which accelerates the corrosion process.

The alloy surface did not show any change after immersion in gasoline. The composition of gasoline did not alter after the immersion tests.

The alloys immersed in sodium chloride solution showed generalized corrosion besides the pits presence.

Zhang and Zhu [4] related that the Fe–25Mn–5Al steel showed no passivation, corrosion potential of −724 V and a corrosion current density of 11.5 μA cm^{-2} in 3.5% NaCl solution. Zhang and Zhu [4] also reported that after the polarization test in NaCl solution, a number of pits were observed on the specimen surface of Fe–25Mn–5Al steel. It is expected that the Fe–Mn base steels may be prone to pitting in chloride ion environments.

In the surface of the FMA alloy with 6.59 wt.% Al was identified, using a EDS analysis, a white area that presented a higher Al and Si content than the concentration in alloy (Fig. 4). The corrosion mechanism of the FMA alloy probably consists of the production of hydrated aluminum oxide, $Al_2O_3{\cdot}H_2O$, and amorphous $SiO_2{\cdot}xH_2O$, which pro-

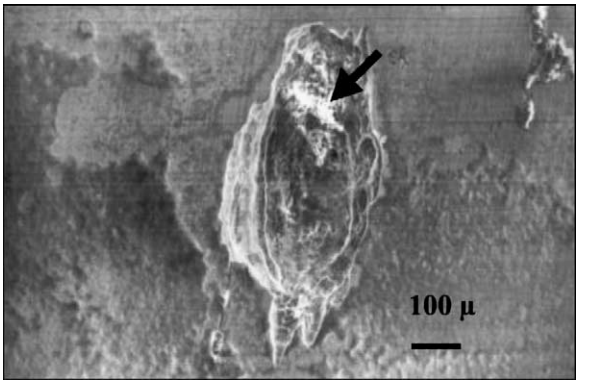

Fig. 4. Surface of the FMA alloy with 0.25% C. The white area presented a higher Al content than the alloy surface.

Table 4
EDS analysis of FMA surface (alloy 1) after immersion in NaCl 3%

Element	Inner area of pit (white) (wt.%)	Inner area of pit (dark) (wt.%)	Surface area (white) (wt.%)	Surface area (dark) (wt.%)
Al	7	2	83	9
Si	1.5	0.6	12	2
Mn	9	22	1.3	33
Fe	2	76	2	54
S	0.03	0.0	0.8	0.2
Cl	–	0.2	0.0	0.6

tects the surface alloy against corrosion. Oh [24] reported that a thin layer containing silicon was formed at the oxide-metal interface to reduce diffusion of metal and oxygen ions in the oxidation of modified high-silicon, low-aluminum Fe–Mn–Si–Al alloys. Silicon plays an important role in the corrosion mechanism of FMA alloys. By adding silicon into the Fe–Mn–Al–C alloys, the oxidation resistance of FMA alloys improved [15]. The oxide layer of the Fe–31.8Mn–6.09Al–1.60Si–0.40C alloy consisted mainly of manganese oxides, which are metal-deficit semiconductors (p-type). Substitution of higher valence cations such as silicon into the lattice of a p-type semiconductor increases the cation vacancy or interstitial anion concentration and decreases the electron hole concentration. Therefore, the diffusion-controlled oxidation rate would be decreased with the incorporation of silicon in the FMA alloys [15]. Aqueous corrosion of FMA alloys, which occurs at ambient temperature, does not involve the silicon diffusion into the manganese oxide lattice, but the production of a protective but discontinuous scale of aluminum and silicon hydrated oxides. Using EDS analysis, it was observed that in the inner area of the pit, the Fe concentration was higher than the alloy composition (Table 4), according to the pitting mechanism. In the inner area of the pit, there was the iron oxidation and the production of Fe^{2+}. The NaCl solution acquired a yellow color, due to the $FeCl_2$ formation, and hydrogen generation was observed. The $FeCl_2$ product suffers hydrolysis to form $Fe(OH)_2$ and H^+ responsible for the hydrogen evolution. The corrosion product was porous and growth in a needle shape perpendicular to the steel surface. Initially, the product was orange and became a dark gray color as the test time increases. Probably, the final corrosion product was $Fe(OH)_3$ or $Fe_2O_3{\cdot}nH_2O$ that becomes darker with the concentration increases.

Table 5
EDS analysis of FMA surface (alloy 2) after immersion in NaCl 3%

Element	Inner area of pit (wt.%)	Surface area (wt.%)
Al	31	11
Si	5	2
Mn	22	30
Fe	40	55
S	0.7	0.0
Cl	0.2	1.1

The corrosion rate was higher for the FMA alloy with the lowest content of aluminum (6.59 wt.% Al). The aluminum corrosion products formed on some areas of the alloy surface probably protect the surface against corrosion. EDS analysis on the surface of alloy 2 showed a sulfur enrichment of the pit area (Table 5). The manganese sulfides accelerated the pitting process because the pH decreased in the inner area of the pit and solubilized the MnS.

In the boiler water, the alloy surface was partially covered with a product, as showed in Fig. 5 (alloy 2 surface). The chemical composition, pH, and dissolved solids of the boiler water used in the immersion

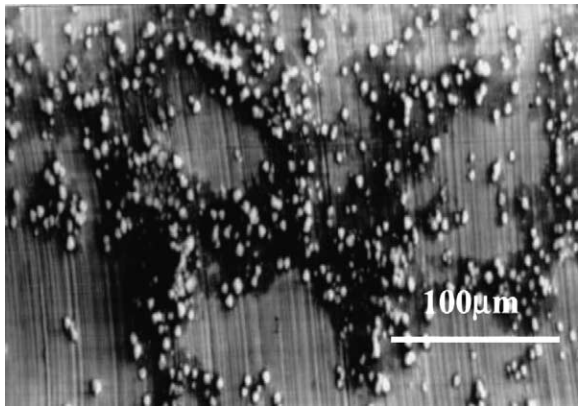

Fig. 5. Surface of Fe–32.3Mn–8.54Al–1.31Si–0.54C alloy after immersion test in boiler water.

Table 6
Chemical analysis of the boiler water

	Before immersion test	After immersion test
pH	6.5	7.3
Soluble Fe (mg L^{-1})	0.18	0.36
Total Fe (mg L^{-1})	0.18	0.54
Mn (mg L^{-1})	<0.40	4
Chlorides (mg L^{-1})	12.5	190.9
SiO_2 (mg L^{-1})	0.20	0.40
Total hardness (mg L^{-1} of $CaCO_3$)	4	6
Dissolved solids (mg L^{-1})	0.003	189

tests were determined (Table 6). After the immersion tests, the concentration of Fe, Mn, and SiO_2 increased. The dissolved solids in solution increased from 0.003 to 189 mg $L^{-}1$. EDS analysis showed an aluminum and silicon enrichment in the white region on the surface of alloy 1 (Table 7). Hydrated aluminum and silicon oxides, $Al_2O_3{\cdot}H_2O$ and amorphous $SiO_2{\cdot}xH_2O$, form an protective scale that decreases the alloy corrosion. Table 8 shows an EDS analysis of the surface of FMA alloy (0.54% C) after immersion in boiler water. The white area of the surface product presented a manganese and calcium concentration higher than the content on the alloy surface, and a lower Fe content than the Fe concentration on the alloy surface. The white region probably contains calcium compounds such as calcium carbonate, manganese compounds such as MnO_2, $Mn_2O_3{\cdot}H_2O$, Mn_3O_4, $MnCO_3$, and $Mn(OH)_2$, products of the possible reactions in the boiler water. Chloride and phosphorus were identified in the dark area of the corrosion product, which showed a higher Ca concentration and a lower Fe concentration than on the surface alloy. In this area, the probable compound $CaCl_2$ could suffer hydrolysis, with the local decrease of pH and the production of $Ca(OH)_2$.

Table 7
EDS analysis of the alloy 1 surface after immersion in boiler water

Element	White area on the alloy surface (wt.%)	Dark area on the alloy surface (wt.%)
Al	67	10
Si	9	4
Mn	4	30
Fe	9	54
S	10	1.5

Table 8
EDS analysis of the alloy 2 surface after immersion in boiler water

Element	Corrosion product (white area) (wt.%)	Corrosion product (dark area) (wt.%)	Alloy surface (wt.%)
Al	2	4	6
Si	1	2	3
Mn	52	38	36
Fe	10	47	53
P	0.0	0.4	0.0
S	0.0	0.2	0.2
Cl	0.0	0.5	0.0
Ca	35	7	2

The FMA alloys immersed in lactic acid suffered attack generalized (Fig. 6). The FMA alloy with 6.59 wt.% was totally corroded. The H_2 generation was intense. The corrosive medium became green. The corrosion product of the FMA alloy with 6.59 wt.% Al was identified as Fe ($C_9H_5O_9$). $3H_2O$ using X-rays diffraction analysis. EDS analysis of the FMA alloy (8.54% Al) surface showed a higher Al content in the white area than the Al concentration on the alloy surface (Fig. 6). In this white area, there was probably a protective scale of aluminum oxides such as the phase $Al_2O_3{\cdot}H_2O$, or aluminum hydroxide, $Al(OH)_3$ (Fig. 6).

The corrosion rates were calculated using the following equation:

$$R = \frac{KW}{AT\rho} \tag{4}$$

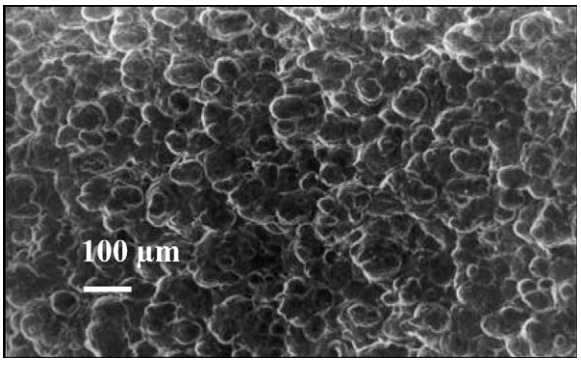

Fig. 6. Surface of Fe–32.3Mn–8.54Al–1.31Si–0.54C alloy after immersion test in lactic acid. The white area was enriched in aluminum in relation to the alloy surface.

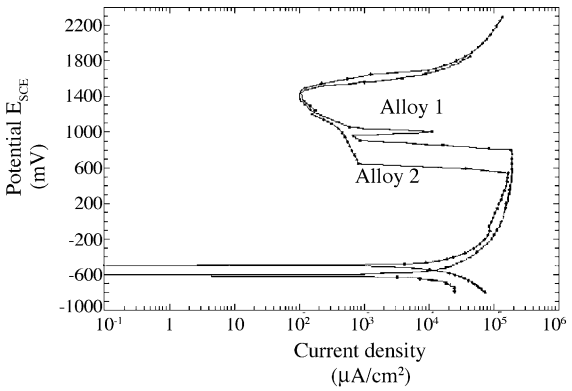

Fig. 7. Polarization curves for Fe–Mn–Al–Si–C alloys in 1N H_2SO_4 solution.

$K = 3.45 \times 10^6$ h cm^{-1} mpy; $T = 480$ h (exposition time); A is the area (cm^2); W the mass loss (g); ρ the density (g cm^{-3}); $\rho_1 = 7.299$ (g cm^{-3}); $\rho_2 = 7.182$ (g cm^{-3}); R the corrosion rate (mpy).

Table 9 presented the average values of the corrosion rates for the two alloys and five environments.

The mass loss was calculated according to the ASTM G1-81 standard.

The FMA alloy with 6.59% Al was totally corroded in lactic acid, and this environment was excluded of the statistical analysis. In the specific case of corrosive environments that produced total mass loss or corrosion rates lower than 1 mpy, the statistical methodology more adequate involves the extreme statistics.

Table 10 showed the corrosion rates used in the statistical analysis for a sample size of 4 and four corrosive media. The freedom degree (FD) of the residue was calculated using the equation:

$$\mathrm{FD} = ab(n-1) - x \quad (5)$$

where x is the estimated data number (Table 11).

Before the hypothesis test, the curves of corrosion rate versus the corrosive environment for the two alloys were done. The absence of parallelism between two curves indicated a possible interaction effect between the corrosive environment and the different chemical composition of the alloy. The effect of the alloy chemical composition on the corrosion rate might depend on the corrosive environment used. A formal statistical hypothesis test was then implemented to verify this possibility. According to the hypothesis test, H_0 is rejected if $F_{obs} > F\alpha$, ν^*, νE, where F_{obs} is the ratio of $MS_{treat.}$ and MS_E, ν^* the degree of freedom associated to the sum of squares of each factor (A and B) and νE the degree of freedom associated to the residue sum of squares.

Considering $\alpha = 0.5\%$: F 0.05, νA, $\nu E = 4.38$, F 0.05, νB, $\nu E = 3.13$.

The hypothesis for the verification of interaction between the factors A (alloy composition) and B (corrosive environment) were:

$$H = (\tau\beta)_{ij} = 0 \,\forall\, ij$$

$$H = \mathrm{one}(\tau\beta)_{ij} \neq 0$$

According to the Table 10, $F_{obs} = 17.3479 > F$ 0.05, νB, $\nu E = 3.13$. Therefore, the hypothesis H_0 was rejected at $\alpha = 5\%$ level and it was concluded that there exists interaction between the alloy composition and the corrosive environments. The effect of the alloy composition in the corrosion rate depends on the corrosive environment. The statistical test confirmed the evidence obtained through the graphic of corrosion rate versus the corrosive environment for the two alloys. Although the presence of interaction between the two factors indicates that their effects on the mean corrosion rates should be studied jointly, sometimes it is also instructive to verify the existence of effect of each factor separately. This statistical test was first

Table 9
Corrosion rates (mpy) after the immersion tests

Corrosive media	Alloy 1 (6.59 wt.% Al)	Alloy 2 (8.54 wt.% Al)
Alcohol	0.5697	0.4891
Gasoline	0.5477	0.9471
3 wt.% NaCl	5.1564	4.4905
Boiler water	4.5395	2.5158
Lactic acid	–	161.2333

Table 10
Corrosion rates (mpy) used in the statistical analysis

Alloy	Corrosive media			
	Alcohol	Gasoline	3 wt.% NaCl	Boiler water
1	0.5697	0.5259	4.4049	4.3682
	0.7472	0.5182	5.3647	4.7107
	0.5489	0.6911	5.1314	4.5395
	0.4129	0.4555	5.7237	4.5395
2	1.2566	0.6797	4.3877	2.8608
	0.2241	0.9049	4.5932	2.4465
	0.1993	0.7939	4.4905	2.5411
	0.2763	1.4100	4.4905	2.2586

Table 11
Variance analysis

Source of variation	Sum of squares	Degrees of freedom	F_{obs}
Factor A (alloy composition)	$SS_A = 2.7844$	$(a-1) = 1$	22.1688
Factor B (corrosive environment)	$SS_B = 107.096$	$(b-1) = 3$	284.1473
Interaction	$SS_{AB} = 6.5368$	$(a-1)(b-1) = 3$	17.3479
Error	$SS_E = 2.385$	$ab(n-1) - 5 = 19$	
Total	$S_T = 118.8035$	$abn - 1 = 31$	

implemented for factor A (alloy composition). The hypothesis used was:

$H_0 = \tau_1 = \tau_2 = 0$

(no effect of alloy composition on the mean corrosion rate)

H_1 : at least one $\tau_i \neq 0$

The results of Table 11 showed that:

$F_{obs} = 22.1688 > F_{0.05,1,19} = 4.38$

Consequently, at the level $\alpha = 5\%$, there are evidences to reject H_0 and conclude that the alloy composition affects the mean corrosion rate. Very little information concerning the effect of aluminum or manganese on corrosion mechanism of austenitic FMA alloys exists in the literature [4]. The two alloys have the same content of manganese, but different concentrations of aluminum, 6.59 wt.% in the alloy 1 and 8.54 wt.% in the alloy 2. Lowest corrosion rates were observed for the alloy 2 in boiler water, NaCl solution, and lactic acid (Tables 9 and 10). These results are according to the observation that increasing Al content improves the corrosion resistance of the Fe–Mn–Al alloys [4]. Although the standard electrode potential of aluminum (−1.66 V) is more negative to that of manganese (−1.18 V – Mn/Mn^{2+}), its passivity coefficient (0.82) is much higher than the passivity coefficient of manganese (0.13). Alloying with Al can promote the passivation ability, increase the resistance to electrode reaction and form a stable and compact Al_2O_3 film, in appropriate conditions. In FMA alloys, as the Al content increases the current density decreases and the open circuit potential increases to a more noble value [4]. This reveals that the increase in the aluminum concentration enhanced the tendency toward passivation and lowered the corrosion rate. Zhang and Zhu [4] observed that the outermost surface and the main part of the passive film formed on Fe–25Mn–5Al are probably the bound water and a mixture of iron, manganese, and aluminum oxides, respectively. For the factor B (corrosive environment), the equality of the corrosion rates obtained for the four environments may be verified. The hypothesis is:

H_0 : $\beta_1 = \beta_2 = \beta = \beta = 0$

H_1 : at least one $\beta_j \neq 0$

The results of Table 10 showed that:

$F_{obs} = 284.1473 > F_{0.05,3,19} = 3.13$

Therefore, there were no evidences (at 5% level) to reject H_0 and conclude that do not exist equality of B effects, or the corrosive environment affects the corrosion rate of alloy.

Then, the conclusion is that exist an effect of factors A and B. Usually, comparisons between the average of treatments are done in order to find the interaction nature. In this case, the interaction between the factors is significant. The comparison between the factor average could be influenced by the AB interaction. So, the comparison between the average of one factor can be done for a fixed level of another factor, through the Turkey test. Initially, the levels of the corrosive environment (factor B) were fixed:

$B = 1$ (alcohol), $Y_{11} = 0.5697$,

$Y_{21} = 0.4891 (0.5697 - 0.4891) = 0.0806$,

$$q_{a,\nu E,a}\left(\frac{\mathrm{MSE}}{n}\right)^{1/2} = q_{2,19,0.05}\left(\frac{0.1256}{4}\right)^{1/2} = 0.5245$$

Considering that $0.0806 < 0.5245$, it was concluded that for the alcohol medium, the average corrosion rates of the two alloys were not (statistically) different. For the alcohol medium, the mass loss was no adequate for distinguish between the corrosion resistance of the two alloys. The mass loss cannot be used as the only

corrosion evaluation method because the alloys showed localized corrosion after immersion in alcohol fuel.

$$B = 2\,(\text{gasoline}), \qquad Y_{12} = 0.5477,$$
$$Y_{22} = 0.9471|0.5477 - 0.9471| = 0.3994,$$
$$q_{a,\nu E,\alpha}\left(\frac{\text{MSE}}{n}\right)^{1/2} = q_{2,19,0.05}\left(\frac{0.1256}{4}\right)^{1/2} = 0.5245$$

Considering that $0.3994 < 0.5245$, it was concluded that for the gasoline medium, the average corrosion rates of the two alloys were not statistically different.

$$B = 3\,(3\%\,\text{NaCl}), \qquad Y_{13} = 5.1564,$$
$$Y_{23} = 4.4905(5.1564 - 4.4905) = 0.6659,$$
$$q_{a,\nu E,\alpha}\left(\frac{\text{MSE}}{n}\right)^{1/2} = q_{2,19,0.05}\left(\frac{0.1256}{4}\right)^{1/2} = 0.5245$$

Considering that $0.6659 > 0.5245$, it was concluded that for the 3% NaCl medium, the average corrosion rates of the two alloys were statistically different.

$$B = 4\,(\text{boiler water}), \qquad Y_{14} = 4.5395,$$
$$Y_{24} = 2.5158(4.5395 - 2.5158) = 2.0127,$$
$$q_{a,\nu E,\alpha}\left(\frac{\text{MSE}}{n}\right)^{1/2} = q_{2,19,0.05}\left(\frac{0.1256}{4}\right)^{1/2} = 0.5245$$

Considering that $2.0127 > 0.5245$, it was concluded that for the boiler water medium, the average corrosion rates of the two alloys were statistically different.

Using the same procedure and fixing the levels of the alloy composition (factor A), the results obtained were that, for the alloy 1 (6.59 wt.% Al), the average corrosion rates were equal for the alcohol and gasoline media, and different for the alcohol and NaCl solution, alcohol and boiler water, gasoline and NaCl solution, gasoline and boiler water, and for NaCl solution and boiler water. In the case of the comparison of the corrosion rates of alloy 1 in the environments NaCl solution and boiler water, the difference $(Y_{13} - Y_{14})$ was very close to the comparison value. So, the least significant difference test (LSD) was applied, and it was concluded that the average values were different.

Using the same statistical procedure for the alloy 2 (8.54 wt.% Al), the conclusions obtained were that the average corrosion rates were equal for the alcohol and gasoline environments, and were different in the following media: alcohol and NaCl solution, alcohol and boiler water, gasoline and NaCl solution, gasoline and boiler water, and between NaCl solution and boiler water. In the verification of the adequacy of the model applied, the followed graphics were done using MINITAB software: (a) residuals versus fitted values for the verification of the equality of variances, (b) residuals versus independent variables (levels of factors A and B) for the verification of residuals dependence on the independent variables and verification of variance equality in the treatments, (c) normal probability plot of the residuals for verification of the normality assumption. All the model assumptions were valid and we can rely on the results of the statistical analysis. Using Eq. (1) and $n = 4$, $b = 4$, $a = 2$, $\sigma = 0.9253$, and $D = 1$, the values of 4.32 and 2.08 for ϕ^2 were obtained. The value read for β was 0.20. The corrosive environment of lactic acid was excluded of the statistical analysis. So, the value of b changed from 5 to 4 (four corrosive environments) and the probability to accept H_0, when H_0 is false increased from 11 to 20%.

3.1.1. Second stage of tests

Table 12 showed the corrosion rates of FMA alloys obtained in the second stage of corrosion tests. The alloy 2 that presented the highest aluminum content showed the highest corrosion rates in sulfuric acid solution.

The steel samples immersed in H_2SO_4 showed generalized corrosion, with intense H_2 generation.

The corrosion rates of the immersion tests were calculated using the Eq. (4).

Table 12
Corrosion rates (mpy) of FMA alloys obtained in the second stage of corrosion tests

Alloy	Potentiostatic method – 1N H_2SO_4	Total immersion test – 1N H_2SO_4
1	3057	15769
	3792	16822
	4896, 4195	17048
Average value	3985	16546
Standard deviation	768.7	682.6
2	11519, 10688	59739
	9478	64030
	13864	49760
Average value	11387	57843
Standard deviation	1852	7321

Table 13
Electrochemical data of the FMA alloys in 1N H_2SO_4 solution

Alloy	E_{corr} (SCE) (mV)	I_{corr} (mA cm^{-2})	E_{cr} (SCE) (mV)	I_{pass} (mA cm^{-2})	E_t (SCE) (mV)	I_{cr} (mA cm^{-2})	R_{corr} (mpy)
1	−610	8.5	960	0.43	1525	188	3985
2	−528	24.0	643	0.45	1550	203	11387

The electrochemical data obtained using the potentiostatic method were showed in Table 13. The corrosion rates of the FMA alloys were calculated using the corrosion current density and the Faraday's law.

At the level $\alpha = 5\%$, for the 1N H_2SO_4 medium, the average corrosion rates of the two alloys were statistically different.

Table 13 showed that the corrosion potential increased with increasing aluminum content of alloy. The alloys showed a tendency towards passivation with high critical current density of about 1.88×10^5 μA cm^{-2} (alloy 1) and 2.03×10^5 μA cm^{-2} (alloy 2). Zhang and Zhu [4] reported a high critical current density (10^5 μA cm^{-2}) for the passivation of Fe–25Mn–5Al in the 1 mol L^{-1} Na_2SO_4 solution. The passive region from 643 to 1550 mV was observed for the Fe–32.3Mn–8.54Al–1.31Si–0.54C alloy. The polarization curve of alloy 1, with 6.59 wt.% Al showed a passive region from 960 to 1525 mV, and a current peak in this potential region. The passive current density was 430 μA cm^{-2} (alloy 1) and 450 μA cm^{-2} (alloy 2). Zhang and Zhu [4] obtained a passive current density of about 150 μA cm^{-2} for the passivation of Fe–25Mn–5Al in HNO_3. The current density decreased due to the production of a protective film of manganese, aluminum and iron oxides [4]. Aluminum has high reactivity among the alloy elements and probably formed a protective aluminum oxide near the metal-oxide interface [15]. As the aluminum was depleted, the plentiful metal oxides (iron and manganese oxides) were formed. The current peak in the passivation region is a result of the scale spalling (Fig. 7). The passive film produced on the surface of alloy with 6.59 wt.% Al contains less protective aluminum oxide than the scale formed on the surface of alloy 2, with 8.54 wt.% Al. The decrease in Al oxides is likely to be responsible for the decreased stability of the passive film.

The corrosion current density was measured using cathodic polarization measurements in the Tafel region (E_{corr} −300 mV). The corrosion current density was 8.5 mA cm^{-2} for the alloy 1 (6.59 wt.% Al) and was 24.0 mA cm^{-2} for the FMA alloy with 8.54 wt.% Al. Zhang and Zhu [4] related that the addition of about 5 wt.% Al to Fe–25Mn steel causes an increase in I_{corr} in 30 wt.% HNO_3 solution. Increasing the concentration of HNO_3 up to 50 wt.%, the Fe–25Mn–5Al alloy showed a corrosion current density lower than the I_{corr} of the Fe–25Mn alloy. The boundary for protective aluminum oxide formation probably tends to higher H_2SO_4 concentrations. The corrosion current density of the alloy with 8.54 wt.% Al could be lower than the I_{corr} of the alloy with 6.59 wt.% Al in more concentrate H_2SO_4 solutions.

As mentioned above, although the standard electrode potential of aluminum (−1.66 V) is more negative to that of manganese (−1.18 V – Mn/Mn^{2+}), its passivity coefficient (0.82) is much higher than the passivity coefficient of manganese (0.13). Alloying with Al can promote the passivation ability, increase the resistance to electrode reaction and form a stable and compact Al_2O_3 film, in appropriate conditions. In FMA alloys, as the Al content increases the current density decreases and the open circuit potential increases to a more noble value [4]. This reveals that the increase in the aluminum concentration enhanced the tendency toward passivation and lowered the corrosion rate.

4. Conclusions

The Fe–Mn–Al–Si–C alloys studied showed low corrosion resistance in the environments sulfuric and lactic acid, boiler water, and NaCl solution.

The corrosion rates of the FMA alloy with lowest content of aluminum (6.59% w/w) were higher than the corrosion rates of the FMA alloy with 8.54% (w/w) Al, in the environments boiler water, NaCl solution, and lactic acid. According to the statistical analysis, applying Two-Way Analysis of Variance with fixed effects, the environments gasoline and fuel alcohol

showed the same corrosivity. However, the alloys immersed in alcohol presented localized corrosion.

Interaction between the alloy and the corrosive environment was identified.

The Analysis of Variance with fixed effect model was valid for the results of the first stage of immersion tests. All the model assumptions were verified.

Potentiotastic tests in H_2SO_4 1N medium showed that the corrosion potential increased with increasing aluminum content of alloy. The alloys showed a tendency towards passivation, with high critical current density of about 1.88×10^5 μA cm^{-2} (alloy 1) and 2.03×10^5 μA cm^{-2} (alloy 2). The passive region from 643 to 1550 mV was observed for the Fe–32.3Mn–8.54Al–1.31Si–0.54C alloy. The polarization curve of alloy 1, with 6.59% (w/w) Al, showed a passive region from 960 to 1525 mV, and a current peak in this potential region. The passive current densities were 430 μA cm^{-2} (alloy 1), and 450 μA cm^{-2} (alloy 2).

References

[1] V.F.C. Lins, E.M. Paula e Silva, Met. ABM 44 (1988) 1265.
[2] G.C.G. Queiroz, P.R. Cetlin, E.M., Paula e Silva, in: Seminário sobre metalurgia física e tratamentos térmicos.COMFIT 7, 51, Associação Brasileira de MetalurgiaBM, São Paulo, 1986.
[3] J.R. Mitchel, M.E. Porter, US Patent 3,201,280 (1965).
[4] Y.S. Zhang, X.M. Zhu, Corros. Sci. 41 (1999) 1817.
[5] Metals Handbook, vol. 13, ASM international, Metals Park, 1987.
[6] C.J. Altstetter, A.P. Bentley, J.W. Fourie, A.N. Kirkbride, Mater. Sci. Eng. 82 (1986) 13.
[7] R. Wang, F.H. Beck, Met. Prog. (1983) 72.
[8] J.G. Duh, L.W. Lee, C.J. Wang, J. Mater. Sci. 23 (1988) 2649.
[9] P.R.S. Jackson, G.R. Wallwork, Oxid. Met. 21 (1984) 47.
[10] J.C. Garcia, N. Rosas, R.J. Rioja, Met. Prog. 124 (1982) 47.
[11] J.G. Duh, C.J. Wang, J. Mater. Sci. 25 (1990) 2063.
[12] S.K. Banerji, Met. Prog. (1978) 59.
[13] J.S. Dunning, M.L. Glenn, H.W. Leavenworth Jr., Met. Prog. (1984) 19.
[14] J. Charles, A. Berghezan, A. Lutts, P.L. Dancoisne, Met. Prog. 119 (1981) 71.
[15] V.F.C. Lins, M.A. Freitas, E.M. Paula e Silva, Corros. Sci. 46 (8) (2004) 1895.
[16] J.S. Chou, C.G. Chao, Scripta Metall. Et Mater. 26 (1992) 1417.
[17] T. Wen, B. Jing, T. Ju, J. Mater. Sci. 22 (1987) 3517.
[18] S.C. Tjong, Surf. Coat. Tech. 28 (1986) 181.
[19] S.T. Shin, C.Y. Tai, T.P. Perng, Corrosion 49 (1993) 130.
[20] M. Ruscak, T.P. Perng, Corrosion 51 (1995) 738.
[21] J.J. Heger, J. Testing Eval. 13 (1985) 447.
[22] D.C. Montgomery, Design and Analysis of Experiments, 5th ed. Wiley, New York, 2000.
[23] A.C.A. Resende, A.B. Landim, G.C. Godoy, E.A. Villegas, in: Congresso Anual da Associação Brasileira de Metais, 45, ABM, Rio de Janeiro, 1990.
[24] J.M. Oh, J. Eletrochem. Soc.: Brief Commun. (1987) 3209.